RSC Advances

ROYAL SOCIETY OF CHEMISTRY

www.rsc.org/advances

View Article Online
DOI: 10.1039/C4RA03289F

Graphical Abstract

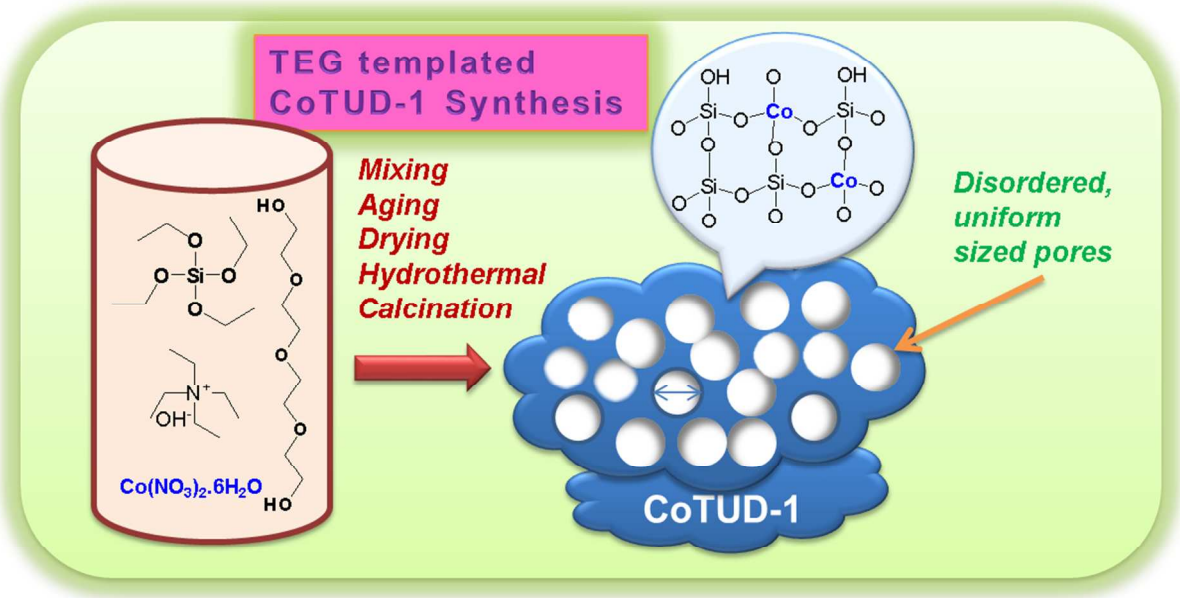

Exclusive Co^{2+} incorporated into the framework of TUD-1 type silicate was obtained using tetraethylene glycol (TEG) as a non-surfactant structure directing agent which are shown to be active for ethylbenzene oxidation.

View Article Online
DOI: 10.1039/C4RA03289F

Cite this: DOI: 10.1039/x0xx00000x

Direct glycol assisted synthesis of amorphous mesoporous silicate with framework incorporated Co^{2+}: characterization and catalytic application in ethylbenzene oxidation

Received 00th January 2012,
Accepted 00th January 2012

DOI: 10.1039/x0xx00000x

www.rsc.org/

Muthusamy P. Pachamuthu [a], Rajamanickam Rajalakshmi [a], Rajamanickam Maheswari [a]* and Anand Ramanathan [b]*

Cobalt was successfully incorporated into an amorphous disordered mesoporous silica, TUD-1 using tetraethylene glycol (TEG) as a non-surfactant structure directing agent. The Si/Co ratio was varied (100, 50 and 25) and the prepared materials were characterized by various analytical and spectroscopic techniques, *viz*., XRD, N_2 sorption, diffuse reflectance UV-Vis, FTIR, ICP-OES, SEM-EDAX, TEM, TGA and XPS studies. N_2 sorption and TEM revealed amorphous mesoporous nature of these materials. The exclusive formation of framework incorporated Co^{2+} species in these materials were confirmed from XPS and UV-Vis studies. Activity of CoTUD-1 material was tested for the liquid phase ethylbenzene oxidation with TBHP (70%) as an oxidant. Various reaction parameters such as time, TBHP concentration and solvents were studied.

Introduction

Co containing catalysts were extensively studied in a variety of organic transformations.[1-6] Due to inherent disadvantages associated with the cobalt salts and homogenous cobalt complexes, heterogeneous cobalt catalysts have been developed to accomplish greener chemical routes. Since the discovery of mesoporous materials, incorporation of Co^{II} in to various mesoporous silicates such as CoMCM-41,[7,8] CoSBA-15,[9] CoSBA-16,[10] CoSBA-1,[11] CoHMS[12] via direct hydrothermal synthesis method and by other methods such as grafting, impregnation have been investigated. All these materials were shown to be catalytically active for a variety of reactions.[13-18] However, the challenging task in these kind of materials are the sustainment of framework incorporated divalent cobalt species[19] and the loss of long range mesoporous structural ordering with increasing loading of Co. Therefore, it is important to develop a synthesis method to accommodate more cobalt species into the silica lattice with the retention of mesoporosity.

We have been preparing metal incorporated disordered mesoporous silicates (TUD-1) via simple, one-pot hydrothermal synthesis method[20-27] and were shown to be catalytically active compared to ordered mesoporous materials. Though, the mechanism of mesopore formation in TUD-1 (non-surfactant - aggregated route) is quite different from the ordered mesoporous silicas (surfactant - micelle route), these materials can incorporate a higher amounts of active M^{x+} species with relatively similar pore size distributions[28, 29]. Recently, large sized metal ions of W[30], Hf[31], Mo[32] and Sn[22] were shown to be incorporated into the TUD-1 porous networks.

Earlier, CoTUD-1[33-36] was prepared using triethanolamine (TEA) as non-surfactant template and was shown to be highly active for cyclohexane oxidation with a higher mono-oxygenated product selectivity compared to other MTUD-1.[37,38] Besides, no leaching of cobalt species was noticed. Moreover, CoTUD-1 materials revealed an excellent *trans*-stilbene epoxidation activity than CoMCM-41, CoX faujasite and Co_3O_4 materials without Co leaching.[39] The superior catalytic activity of CoTUD-1 was attributed to a higher amount of isolated Co(II) species. The higher Co dispersion was further ascribed to the M-atrane routed synthesis mechanism of TUD-1 enabled by the structure directing agent TEA.[28]

In a similar role organic molecules such as tetraethylene glycol (TEG) can also be applied for the TUD-1 synthesis. Shan *et al* has used TEG successfully as a template and obtained very stable, amorphous high surface area (~530 m^2/g) mesoporous alumina with TUD-1 structure.[40] Likewise, TEG template method retained more of Al^{3+} incorporations (Si/Al = 4) in the AlTUD-1 synthesis.[41] These results further directed our focus on the TEG routed MTUD-1 synthesis. Recently, we have reported MnTUD-1 and ZrTUD-1 materials by adopting TEG templating method[21,26] which accomplished presence of more isolated M^{x+} species in the walls of mesoporous silica. In the present investigation, Co incorporated TUD-1 materials are synthesized using TEG as structure directing agent. These materials are well characterized by XRD, N_2 sorption, XPS, DR-UV-Vis, FTIR, ICP-OES, SEM and TEM. The catalytic performance of CoTUD-1 is investigated for liquid phase ethylbenzene oxidation in the presence of TBHP oxidant.

View Article Online
DOI: 10.1039/C4RA03289F
ARTICLE Journal Name

Experimental

Catalyst synthesis

The synthesis of CoTUD-1 with Si/Co ratio of 100, 50, and 25 has been carried out comparable to that of ZrTUD-1.[21] A clear synthesis mixture with a molar ratio composition of 1 SiO_2: (0.01 - 0.04) Co: 0.5 TEAOH: 1 TEG: 11 H_2O was prepared by adding a solution of cobalt salt ($Co(NO_3)_2.3H_2O$, Merck) in 2 mL of deionized water to 21.2 g of tetraethyl orthosilicate (TEOS, Sigma-Aldrich) and stirring for few minutes. Then, a mixture of 14 g of tetraethylene glycol (TEG, SRL) with 3 mL of deionized water was added drop wise, and stirred for 1 h. Finally 19.8 g of tetraethylammonium hydroxide (TEAOH, 35%, Sigma-Aldrich) was added. The obtained gel was aged at room temperature for 24 h, dried at 100°C for 24 h and autoclaved for hydrothermal treatment at 160°C for 8 h. The synthesized solid was calcined at 600 °C for 10 h at a rate of 1 °C/min in the presence of air and the prepared samples are denoted as CoTUD-1(X) where X represents Si/Co ratio.

For catalytic comparative purposes, TEA templated disordered mesoporous materials like TiTUD-1(50)[42], CrTUD-1(50)[28] and CTAB templated ordered mesoporous CoMCM-41(50)[42], were also synthesized as per reported procedures. The number in parenthesis denotes the Si/M ratio.

Characterization

Powder X-ray diffraction (XRD) measurements were carried out on a Rigaku diffractometer with a nickel filtered Cu Kα (λ = 1.5418 Å) radiation source. The surface area, pore volume and pore size distribution were evaluated from nitrogen sorption carried out at −196 °C using a Quantochrome porosimeter (Quadrasorb*SI*). The sample was degassed at 250 °C for 2 h before the measurement. Transmission electron microscopy (TEM) was performed on FEI Tecnai G2 fitted with a CCD camera. The sample morphologies were examined using high resolution scanning electron microscope (HR-SEM) - FEI Quanta FEG 200 with low vacuum mode operation. Diffuse reflectance UV-Vis spectra were recorded in the range of 200–800 nm with Thermoscientific Evolution 600 equipment with diffuse reflectance attachments, using $BaSO_4$ as a reference. FTIR spectra of KBr-diluted pellets of the sample were recorded on a Bruker instrument at room temperature with a resolution of 4 cm^{-1} averaged over 100 scans. The X-ray photoelectron spectroscopy (XPS) spectra were carried out by using an Omicron ESCA probe spectrometer with Al Kα X-rays (*hν* =1486.6 eV) radiation. Elemental analysis was determined by inductively coupled plasma-optical emission spectroscopy (ICP-OES) on a Perkin Elmer OES Optima 5300 DV spectrometer. Thermal analysis (TGA) was performed using a SDT Q600 (TA Instruments, Inc.,) thermal analyzer system under N_2 atmosphere (100 ml/min) with a heating rate of 10 °C/min.

Ethylbenzene oxidation

Liquid phase oxidation of ethylbenzene was carried out in one neck reaction tube fitted with temperature controlled oil bath. Typically, 10 mmol of ethylbenzene, 10 mmol of TBHP (70 wt %), 0.1 g of CoTUD-1 catalyst were added to the 10 ml of acetonitrile solvent in the reaction tube. Then preactivated catalyst (250 °C, 3h) was added and the reaction tube is heated to 80 °C under vigorous stirring. After a certain time, the mixture was cooled to room temperature. The catalyst was allowed to settle to the bottom of the tube and the liquid product was filtered from the solid catalyst. The liquid products were then analyzed on a Shimadzu GC-2010, AOC-20i (Autoinjector) gas chromatography instrument with Restek 5 column. The products were identified on a GC-MS (Agilent Technologies 6850 N series with a HP-5 capillary column) analysis.

Results and Discussion

Characterization of CoTUD-1 materials

Low angle powder XRD patterns of CoTUD-1 with different Si/Co ratios (Figure 1) showed a broad single reflection in the low angle region between 0.5-1.5 2θ° similar to those reported for TUD-1 type materials.[21,26,33] These types of low angle broad reflections were also observed for the KIT-1 and MSU-1 type disordered mesoporous silica.[43,44] These peaks are indicative of disordered mesoporous nature of CoTUD-1 materials which are further ascertained from the N_2-sorption analysis (Figure 2a). A type IV isotherm with H2 hysteresis loop was observed for all samples, signifying that the mesopores are indeed interconnected and disordered as well.

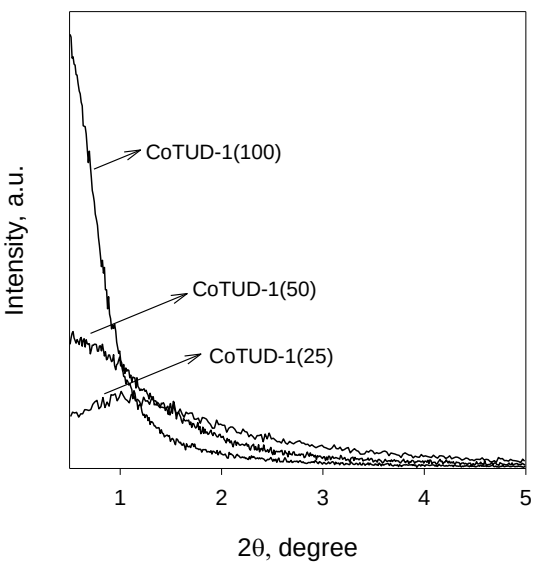

Figure 1. Low angle XRD of CoTUD-1 with different Si/Co ratio

The pore size distribution obtained from the adsorption isotherm (Figure 2b) showed a relatively broader pore distribution compared to those obtained by TEA template

View Article Online
DOI: 10.1039/C4RA03289F

synthesis. Nevertheless, the average pore diameter was observed to be in the range of 4.5-6.5 nm (Table 1). On the other hand, the surface area (564-628 m^2/g), and pore volume (0.67-0.77 cm^3/g) were observed to be very close to that of CoTUD-1 materials prepared using TEA [33, 35] with no significant effect on Co loading (Table 1).

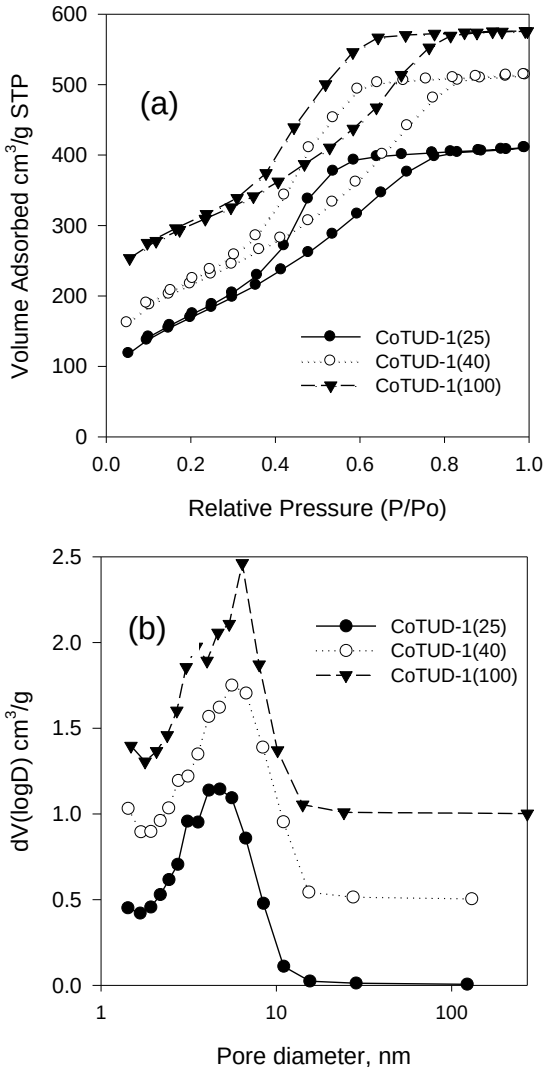

Figure 2. (a) N2 sorption and (b) pore size distributions of CoTUD-1 with different Si/Co ratio.

Table 1. Textural properties of CoTUD-1

CoTUD-1 (Si/Co)	Si/Co (molar ratio)		S_{BET}[b]	$V_{p,BJH}$[c]	$d_{P,BJH}$[d]
	Synthesis gel	Calcined[a]	m^2/g	cc/g	nm
100	100	101	564	0.71	6.3
50	50	42	622	0.77	5.5
25	25	28	628	0.67	4.6

[a] Elemental analysis by ICP-OES. [b]S_{BET} = Specific surface area. [c]$VP_{,BJH}$ = Total pore volume at P/Po = 0.98. [d]$dP_{,BJH}$= BJH adsorption pore diameter

Elemental analysis (ICP-OES) results showed that the Si/Co molar ratio obtained after calcinations is close to that in the synthesis gel (Table 1) implying that all the added Co were incorporated in the final solid samples. SEM image of CoTUD-1 sample revealed an uneven foams or spherical shapes with different particle sizes (Figure 3a and b). The EDAX spectrum of CoTUD-1(25) indicated the presence of Si, O, and Co elements with an average estimate of 4.5 wt.% cobalt which is close to the Si/Co molar ratio estimated from ICP-OES (Figure 3c). The disordered foam or wormhole type pores of CoTUD-1[21,26,28,33] is further confirmed by transmission electron micrograph (Figure 3d).

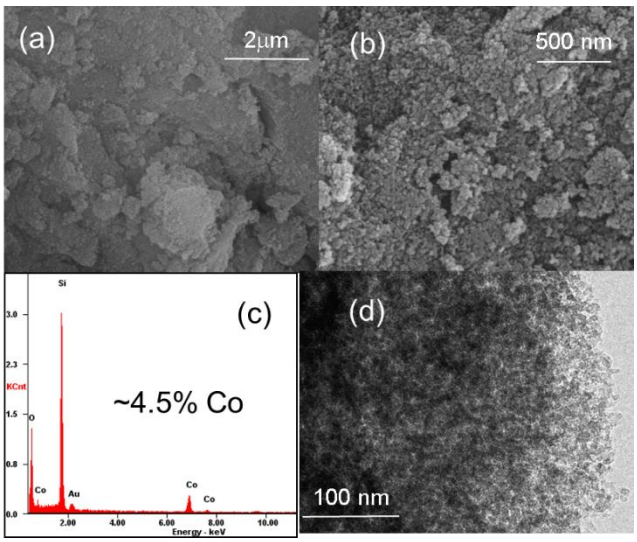

Figure 3. SEM micrographs at different magnification (a and b), corresponding EDX analysis (c) and TEM image of CoTUD-1(25).

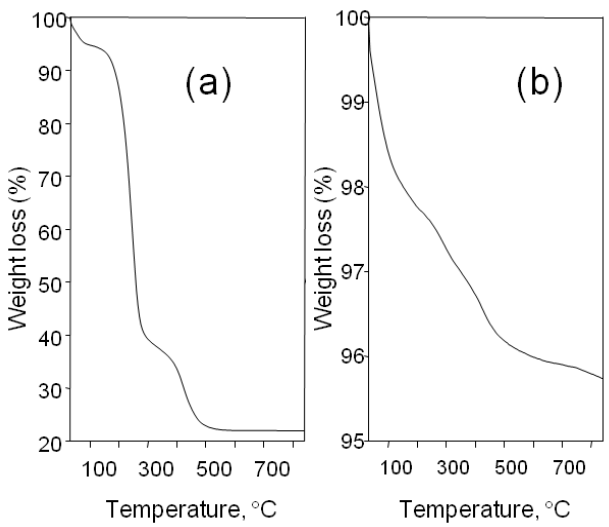

Figure 4. TGA curves of (a) as-synthesized and (b) calcined CoTUD-1(50) sample.

Thermogravimetric analysis (TGA) of as-synthesized and calcined CoTUD-1(50) is depicted in Figure 4. A total weight loss of ~80% corresponding to the removal of adsorbed water and ethanol molecules (5-7%, <170 °C), removal of template molecules (53%, 170-300 °C) which

View Article Online
DOI: 10.1039/C4RA03289F
Journal Name

includes TEG and TEA^+ (TEA^+OH^-) and finally the removal of surface Si-OH groups and strongly bound organic moieties (23%, 300-500 °C) were noticed. On the other hand, TGA of calcined CoTUD-1(50) showed around 4 % weight loss, which could be attributed to the removal of adsorbed water (strongly bonded) present within the mesopores proving the thermal stability of TUD-1 type materials.

Wide angle XRD patterns of CoTUD-1 (Figure 5) showed only a broad diffraction peak in the 2θ range of 10-30°, due to amorphous nature of silica. no reflections corresponding to crystalline cobalt oxide (Co_3O_4 2θ – 37, 45, 65°)[8] were noted indicating that all cobalt species appears to be framework incorporated; and, if any cobalt oxide is formed, it might be dispersed homogeneously in the mesopore channels of TUD-1

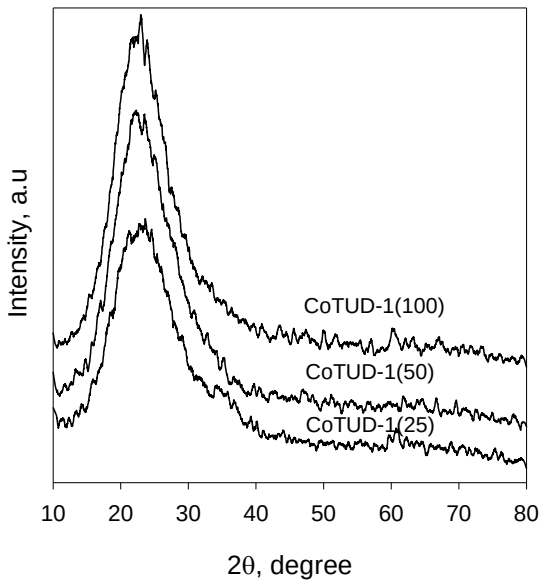

Figure 5. Wide angle XRD of calcined CoTUD-1 with different Si/Co ratio.

The FT-IR spectra of calcined CoTUD-1 in the range of 4000–500 cm^{-1} are displayed in Figure 6. The broad band around ~3460 cm^{-1} is mainly caused by the O–H stretching vibration of the adsorbed water molecules or surface silanol groups (Si-O-H) and their bending vibration mode is observed at 1640 cm^{-1}. The intense vibration bands observed at 1238, 1087 and 804 cm^{-1} are due to the asymmetric and symmetric stretching vibrations of Si–O–Si bond.[22] The absorption band at 962 cm^{-1} is attributed to stretching vibration of Si–O units bound to heteroatoms (Co or H).[21,22,30]

We have assessed diffuse reflectance UV-Vis in order to investigate the local environment of cobalt ions in the calcined CoTUD-1 samples which showed three peaks in the visible region (Figure 7). The absorbance in the range of 500–700 nm is characteristics for tetrahedrally coordinated Co^{2+}.[33,45,46] In general, the cobalt modified mesoporous materials showed tetrahedral Co^{2+} in the silica framework at 523, 580, and 652 nm, which can be assigned to the $^4A_2(F) \rightarrow {}^4T_1(P)$ transition of Co(II) ion.[10,39,45-47]. These characteristic peaks were also observed in CoTUD-1 samples. As-synthesized CoTUD-1(50) sample showed absorbance bands at 475 and 508 nm due to the Co^{2+} ions octahedral environment.[10,33,39,45] However, absence of these bands in calcined samples clearly evident the complete tetrahedral incorporation of Co^{2+}. In addition, no characteristic Co_3O_4 absorbance bands were observed in CoTUD-1 samples and are in line with high angle XRD observations.

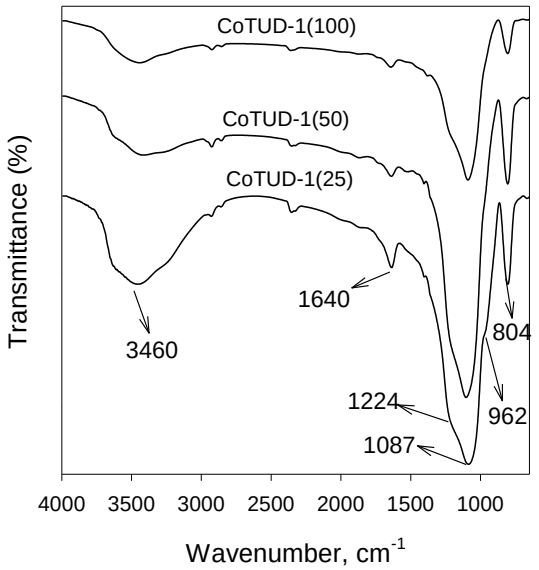

Figure 6. FTIR spectra of calcined CoTUD-1 with different Si/Co ratio.

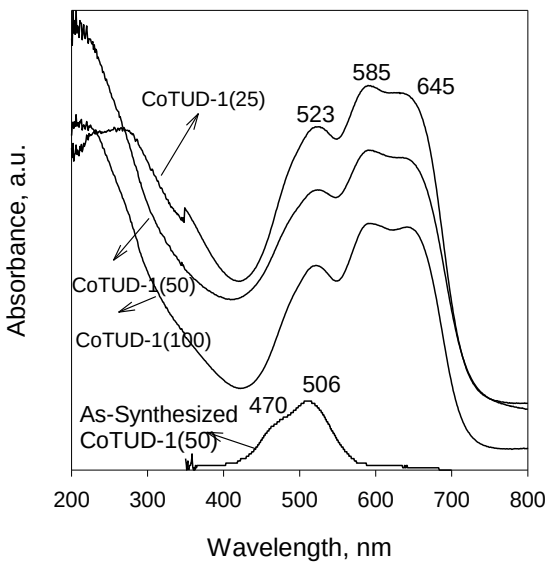

Figure 7. Diffuse reflectance UV-Vis of CoTUD-1.

View Article Online
DOI: 10.1039/C4RA03289F

The oxidation state of cobalt was further investigated by XPS. Figure 8 shows the Co 2p XPS spectra for CoTUD-1(50) which showed binding energy of 799.4 eV (for Co 2p1/2) and 782.1 eV (for Co 2p3/2). Similar binding energy values were reported for ordered mesoporous silicates containing cobalt (CoMCM-41, CoSBA-16, CoHMS), which are assigned to an interaction of tetrahedral Co (II) with the silica wall[48]. In addition, absence of peaks with BE values ~780 eV and 786 eV confirms the absence of Co_3O_4 and CoO (Co(II) octahedral symmetry) species[49]in CoTUD-1. These results are in accordance with XRD and diffuse reflectance UV Vis studies.

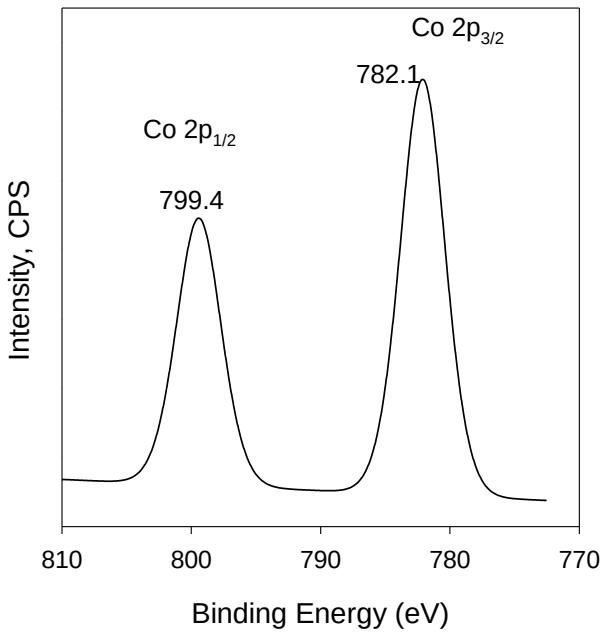

Figure 8. Co 2p XPS spectrum of CoTUD-1(50).

Oxidation of Ethylbenzene over CoTUD-1

The main products of ethylbenzene (EB) oxidation were acetophenone (AP), 1-phenylethanol (1-PE) and benzaldehyde as identified by authentic standards in gas chromatographs. No appreciable catalytic activity was obtained in a blank run with all silica TUD-1 (Table 2). Under our experimental conditions, with CoTUD-1, negligible activity was also obtained with air as oxidant. On the other hand, while using H_2O_2 (30 wt.%) as oxidant 18 % of EB conversion resulting in 44 % AP, 34 % PhCHO and 22 % 1-PE selectivities were noted (Table 2). However, relatively higher conversion of EB (38%) with high selectivity to AP (74%) was obtained when TBHP (70%) was used as oxidant. It is well known that decomposition of TBHP typically proceeds *via* the Haber-Weiss mechanism[50]. The cobalt species (Co^{2+}/Co^{3+}) with its one-electron redox cycles promote the homolytic decomposition of peroxides efficiently even at low Co concentrations by the following pathways (Eq 1 and 2).

$$Co(II) + ROOH \longrightarrow Co(III)OH + RO^{*} \quad \text{(1)}$$

$$Co(III)OH + ROOH \longrightarrow Co(II) + ROO^{*} + H_2O \quad \text{(2)}$$

Table 2. Oxidation of ethylbenzene at 80 °C

Catalyst	Oxidant	EB conv. (%)	Product Selectivity (%)		
			AP	1-PE	PhCHO
SiTUD-1	TBHP	4	88	11	
CoTUD-1(50)	H_2O_2	18	44	22	34
CoTUD-1(50)	TBHP	38	74	17	9

Reaction conditions: Ethyl benzene – 10 mmol, TBHP – 10 mmol, Catalyst – 100 mg, Acetonitrile – 10 ml, Time – 8 h.

The effect of time on EB oxidation over CoTUD-1(50) at 80 °C is presented in Table 3. Though a linear increase in EB conversion was noted in shorter reaction times, prolonging the reaction time to 24h yielded a conversion of 46%, approximately 3 fold increase compared to 1h. On the other hand, product selectivites were varied, for instance, 1-PE's selectivity was observed nearly ~40% after 1h of reaction which decreased with time at the expense of AP formation. This time profile suggest that 1-PE is a primary product and the abstraction of hydrogens from (-OH and –CH of 1-PE) by the activated *t*-butyl hydroperoxide oxygen yields AP[27]. The effect of cobalt content in CoTUD-1 was also studied and reported in Table 4. A marginal increase in EB conversion (31 to 38%) was noted with an increase in Co content with similar product distribution for CoTUD-1(100 and 50) catalysts. On the other hand, AP selectivity decreased drastically from 74% to 61% for CoTUD-1(25) catalyst with an increase in benzaldehyde and benzoic acid formation. These results suggest an optimum amount of ~2mol% Co^{2+} can be effectively catalyze EB oxidation with a high AP selectivity of ~75%.

Table 3. Effect of time on oxidation of ethylbenzene over CoTUD-1(50) at 80 °C

Time (h)	EB conv. (%)	Product Selectivity (%)		
		AP	1-PE	PhCHO
1	14	55	39	6
3.5	29	66	26	8
8	38	74	17	9
24	46	68	14	11(7[a])

Reaction conditions: Ethyl benzene – 10 mmol, TBHP – 10 mmol, Catalyst – 100 mg, Acetonitrile – 10 ml, [a] other products

The ratio of TBHP was varied keeping same amount of EB over CoTUD-1(50) and the results are presented in Table 5. EB conversion was found to increase from 26 to 51% with an increase in TBHP mole ratio from 0.5 to 2. No significant increase in EB conversion (54%) was noted with a further increase in the TBHP amount. This was partially attributed to active sites blockage by excess water from TBHP (70%) thus hindering effective EB conversion[25]. In

View Article Online
DOI: 10.1039/C4RA03289F
ARTICLE Journal Name

addition, benzoic acid was observed (6-8%) at a higher TBHP concentration, due to oxidation of benzaldehyde.

Table 4. Effect of TBHP ratio on oxidation of ethylbenzene over CoTUD-1(50) at 80 °C

TBHP/EB ratio	EB conv. (%)	Product Selectivity (%)		
		AP	1-PE	PhCHO
0.5	26	45	31	24
1	38	74	17	9
2	51	62	18	14
3	54	65	21	6

Reaction conditions: Ethyl benzene – 10 mmol, Catalyst – 100 mg, Acetonitrile – 10 ml, Time – 8 h.

Table 5. Influence of Co loading on oxidation of ethylbenzene at 80 °C

CoTUD-1 (Si/Co)	EB conv. (%)	Product Selectivity (%)		
		AP	1-PE	PhCHO
100	31	75	18	7
50	38	74	17	9
25	43	61	21	14

Reaction conditions: Ethyl benzene – 10 mmol, Catalyst – 100 mg, Acetonitrile – 10 ml, Time – 8 h.

Solvent effect is apparent when the reaction was investigated in different polar protic/aprotic solvents like acetonitrile, ethanol, dichloromethane, DMF and ethyl acetate (Table 6). Among various solvents studied, EB conversion was found to proceed effectively in the following order: ethyl acetate > acetonitrile > DMF > dichlomethane > ethanol. Similar solvent effects were observed for various catalysts (CoMCM-41[48], CoHMS[12], MnTUD-1[27] and CuTUD-1[25]) as well. Due to highly selective AP formation with minimum side products, acetonitrile solvent was preferred for CoTUD-1 catalysts.

Table 6. Effect of solvents on oxidation of ethylbenzene over CoTUD-1(50) at 80 °C

Solvent	EB conv. (%)	Product Selectivity (%)			
		AP	1-PE	PhCHO	Others
Ethanol	2	100	0	0	0
Dichloromethane	16	55	39	-	6
DMF	28	62	10	18	10
Acetonitrile	38	74	17	9	
Ethylacetate	42	71	16	12	10

Reaction conditions: Ethyl benzene – 10 mmol, TBHP – 10 mmol, Catalyst – 100 mg, Acetonitrile – 10 ml, Time – 8h, others – mainly benzoic acid.

Finally the catalytic activity of CoTUD-1 was compared with other metal incorporated TUD-1 (Ti, Cr, Cu, Mn) and cobalt containing ordered mesoporous materials and their results are summarized in Table 7. EB conversion was found to be lower with MnTUD-1 followed by Ti-TUD-1. Similar EB conversion was observed for CuTUD-1 and CoTUD-1. A higher EB conversion was noted for CrTUD-1. Interestingly, Ti-, Mn- and Cu containing TUD-1 catalysts showed lower AP selectivies (60-65%). On the other hand CrTUD-1 produced more of 1-PE possibly due to higher decomposition rate of TBHP compared to other metal ions. A slightly higher EB conversion was observed for Co containing ordered MCM-41catalyst compared to disordered TUD-1 catalysts. Nevertheless, AP yields were found to be nearly same for both Co containing disordered and ordered catalysts.

Further, the reusable ability of the catalyst was established by three recycle runs (Table 8). After each reaction cycle, the catalyst was filtered, washed and activated at 200°C for 2h. The catalyst showed the similar conversion and selectivity with the fresh CoTUD-1 catalyzed reaction. CoTUD-1(50) catalyst was hot-filtered from the reaction mixture and the filtrate was analysed for Co by ICP-OES method. About 4.2 ppm which is about 6% of total Co content in the catalyst was determined in the filtrate. Thus, the recycle studies and hot-filtration experiment signified heterogeneity of EB oxidation with CoTUD-1.

Table 7. Oxidation of ethylbenzene over different metal containing TUD-1 and CoMCM-41 catalysts at 80 °C

Catalysts	EB conv. (%)	Product Selectivity (%)		
		AP	1-PE	PhCHO
MnTUD-1(44)[27]	19.8	60.8	26.6	12.6
TiTUD-1(50)	32	67	23	10
CuTUD-1(50)[25]	36.3	65.3	15.3	16.8
CoTUD-1(50)	38	74	17	9
CrTUD-1(50)	43	10	60	30
CoMCM-41(50)	42	66	19	14

Reaction conditions: Ethyl benzene – 10 mmol, TBHP – 10 mmol, Catalyst – 100 mg, Acetonitrile – 10 ml, Time – 8h.

Table 8. Influence of Co loading on oxidation of ethylbenzene at 80 °C

CoTUD-1	EB conv. (%)	Product Selectivity (%)		
		AP	1-PE	PhCHO
Fresh	38	74	17	9
Second	36	72	20	8
third	31	72	18	10

Reaction conditions: Ethyl benzene – 10 mmol, Catalyst – 100 mg, Acetonitrile – 10 ml, Time – 8 h.

Conclusions

Simple TEG molecule was successfully utilized for Co(II) incorporation into the TUD-1 type structured material with relatively narrow pore size distribution (4.5-6.5 nm) and a surface area of about 600 m^2/g. Diffuse reflectance UV-Vis and XPS studies confirmed the exclusive presence of Co(II) ions in the TUD-1 silica lattice. CoTUD-1 materials converted ethylbenzene (~40 %) to corresponding oxidized products AP, 1-PE and PhCHO in the presence of TBHP

View Article Online
DOI: 10.1039/C4RA03289F

that are attributed to highly dispersed Co^{2+} active sites. The reaction time, EB:TBHP ratio and solvents were mainly influenced the EB conversion and products selectivity. The activity of CoTUD-1 is comparable and similar to that of ordered CoMCM-41 catalyst. Most importantly, no leaching of Co species were observed confirming heterogeneity of this reaction.

Acknowledgements

The author M.P.P. is thankful to DST-FIST and UGC – Research Fellowship scheme. The authors would like to thank Dr. R. Karvembu, Head, Department of Chemistry, National Institute of Technology (NIT), Tiruchirappalli, India for performing the GC analysis.

Notes and references

[a] Department of Chemistry, Anna University, Chennai 600025, India.
[b] Center for Environmentally Beneficial Catalysis (CEBC), The University of Kansas, Lawrence, KS 66047, USA. E-mail: anand@ku.edu; Fax: +1 785 864 6051; Tel: +1 785 864 1631.

1 G. Cahiez and A. Moyeux, *Chem. Rev. (Washington, DC, U. S.)*, 2010, **110**, 1435-1462.
2. X.-B. Lu and D. J. Darensbourg, *Chem. Soc. Rev.*, 2012, **41**, 1462-1484.
3. H. Yorimitsu and K. Oshima, *Pure Appl. Chem.*, 2006, **78**.
4. F. Hebrard and P. Kalck, *Chem. Rev. (Washington, DC, U. S.)*, 2009, **109**, 4272-4282.
5. T. J. Korn, M. A. Schade, S. Wirth and P. Knochel, *Org. Lett.*, 2006, **8**, 725-728.
6. H. Lu, V. Subbarayan, J. Tao and X. P. Zhang, *Organometallics*, 2009, **29**, 389-393.
7. V. Parvulescu and B. L. Su, *Catal. Today*, 2001, **69**, 315-322.
8. Q. Tang, Q. Zhang, H. Wu and Y. Wang, *J. Catal.*, 2005, **230**, 384-397.
9. A. Vinu and M. Hartmann, *Chem. Lett.*, 2004, **33**, 588-589.
10. Y. Dong, X. Zhan, X. Niu, J. Li, F. Yuan, Y. Zhu and H. Fu, *Microporous Mesoporous Mater.*, 2014, **185**, 97-106.
11. A. Vinu, J. Dědeček, V. Murugesan and M. Hartmann, *Chem. Mater.*, 2002, **14**, 2433-2435.
12. S. S. Bhoware, S. Shylesh, K. Kamble and A. Singh, *J. Mol. Catal. A: Chem.*, 2006, **255**, 123-130.
13. M. K. Gnanamani, G. Jacobs, U. M. Graham, W. Ma, V. R. R. Pendyala, M. Ribeiro and B. H. Davis, *Catal. Lett.*, 2010, **134**, 37-44.
14. T. Tsoncheva, L. Ivanova, J. Rosenholm and M. Linden, *Appl. Catal., B*, 2009, **89**, 365-374.
15. H. Cui, Y. Zhang, Z. Qiu, L. Zhao and Y. Zhu, *Appl. Catal., B*, 2010, **101**, 45-53.
16. C. Wang, S. Lim, G. Du, C. Z. Loebicki, N. Li, S. Derrouiche and G. L. Haller, *J. Phys. Chem. C*, 2009, **113**, 14863-14871.
17. Á. Szegedi, M. Popova, V. Mavrodinova and C. Minchev, *Appl. Catal., A*, 2008, **338**, 44-51.
18. R. Nava, B. Pawelec, J. Morales, R. A. Ortega and J. L. G. Fierro, *Microporous Mesoporous Mater.*, 2009, **118**, 189-201.
19. T. Vrålstad, G. Øye, M. Stöcker and J. Sjöblom, *Microporous Mesoporous Mater.*, 2007, **104**, 10-17.
20. M. P. Pachamuthu, V. V. Srinivasan, R. Maheswari, K. Shanthi and A. Ramanathan, *Catalysis Science & Technology*, 2013, **3**, 3335-3342.
21. M. P. Pachamuthu, V. V. Srinivasan, R. Maheswari, K. Shanthi and A. Ramanathan, *Appl. Catal., A*, 2013, **462–463**, 143-149.
22. M. P. Pachamuthu, K. Shanthi, R. Luque and A. Ramanathan, *Green Chem.*, 2013, **15**, 2158-2166.
23. P. Muthusamy Poomalai, R. Anand, S. Kannan and M. Rajamanickam, in *Novel Materials for Catalysis and Fuels Processing*, American Chemical Society, 2013, vol. 1132, ch. 7, pp. 195-211.
24. K. Kandasamy, M. P. Pachamuthu, M. Muthusamy, S. Ganesabaskaran and A. Ramanathan, *Rsc Adv*, 2013, **3**, 25367-25373.
25. R. Maheswari, M. P. Pachamuthu and R. Anand, *J. Porous Mater.*, 2012, **19**, 103-110.
26. R. Maheswari, R. Anand and G. Imran, *J. Porous Mater.*, 2012, **19**, 283-288.
27. G. Imran, M. Pachamuthu, R. Maheswari, A. Ramanathan and S. J. Sardhar Basha, *J. Porous Mater.*, 2012, **19**, 677-682.
28. S. Telalovic, A. Ramanathan, G. Mul and U. Hanefeld, *J. Mater. Chem.*, 2010, **20**, 642-658.
29. J. Wang, J. C. Groen and M.-O. Coppens, *J. Phys. Chem., C*, 2008, **112**, 19336-19345.
30. J. ten Dam, D. Badloe, A. Ramanathan, K. Djanashvili, F. Kapteijn and U. Hanefeld, *Appl. Catal., A*, 2013, **468**, 150-159.
31. L. Li, T. I. Korányi, B. F. Sels and P. P. Pescarmona, *Green Chem.*, 2012, **14**, 1611-1619.
32. M. S. Hamdy and G. Mul, *Catalysis Science & Technology*, 2012, **2**, 1894-1900.
33. M. S. Hamdy, A. Ramanathan, T. Maschmeyer, U. Hanefeld and J. C. Jansen, *Chemistry – A European Journal*, 2006, **12**, 1782-1789.
34. R. Anand, M. S. Hamdy, P. Gkourgkoulas, T. Maschmeyer, J. C. Jansen and U. Hanefeld, *Catal. Today*, 2006, **117**, 279-283.
35. M. S. Hamdy, G. Mul, W. Wei, R. Anand, U. Hanefeld, J. C. Jansen and J. A. Moulijn, *Catal. Today*, 2005, **110**, 264-271.
36. R. Anand, M. S. Hamdy, U. Hanefeld and T. Maschmeyer, *Catal. Lett.*, 2004, **95**, 113-117.
37. A. Ramanathan, M. S. Hamdy, R. Parton, T. Maschmeyer, J. C. Jansen and U. Hanefeld, *Appl. Catal., A*, 2009, **355**, 78-82.
38. R. Anand, M. S. Hamdy, R. Parton, T. Maschmeyer, J. C. Jansen, R. Glaeser, F. Kapteijn and U. Hanefeld, *Aust. J. Chem.*, 2009, **62**, 360-365.
39. X. Y. Quek, Q. H. Tang, S. Q. Hu and Y. H. Yang, *Appl. Catal., A*, 2009, **361**, 130-136.
40. Z. Shan, J.C. Jansen, W. Zhou and Th. Maschmeyer, *Appl. Catal., A*, 2003, **254**, 339–343.
41. C. Simons, U. Hanefeld, I. W. C. E. Arends, T. Maschmeyer and R. A. Sheldon, *Top. Catal.*, 2006, **40**, 35-44.
42. Z. Shan, J. C. Jansen, L. Marchese and T. Maschmeyer, *Microporous Mesoporous Mater.*, 2001, **48**, 181-187.
42. H. T. Gomes, P. Selvam, S. E. Dapurkar, J. L. Figueiredo and J. L. Faria, *Microporous Mesoporous Mater.*, 2005, **86**, 287-294.

View Article Online
DOI: 10.1039/C4RA03289F

43. R. Ryoo, J. M. Kim, C. H. Ko and C. H. Shin, *J. Phys. Chem.*, 1996, **100**, 17718-17721.
44. L. Liu, H. Li and Y. Zhang, *Catal. Today*, 2006, **115**, 235-241.
45. P. Selvam and S. Mohapatra, *J. Catal.*, 2005, **233**, 276-287.
46. H. Ma, J. Xu, C. Chen, Q. Zhang, J. Ning, H. Miao, L. Zhou and X. Li, *Catal. Lett.*, 2007, **113**, 104-108.
47. Á. Szegedi, M. Popova and C. Minchev, *J. Mater. Sci.*, 2009, **44**, 6710-6716.
48. S. S. Bhoware and A. P. Singh, *J. Mol. Catal. A: Chem.*, 2007, **266**, 118-130.
49. P. A. Robles-Dutenhefner, K. A. da Silva Rocha, E. M. B. Sousa and E. V. Gusevskaya, *J. Catal.*, 2009, **265**, 72-79.
50. C. Futter, E. Prasetyo and S. A. Schunk, *Chem. Ing. Tech.*, 2013, **85**, 420-436.